Recent EFT measurements from CMS

Matteo Presilla

3rd General Meeting of the LHC EFT Working Group

What's new*

TOP measurements

TOP-21-001 **tZq/ttZ to multileptons**.

TOP-19-006 Charged LFV.

TOP-20-007 FCNC in tH(γγ).

TOP-19-002 FCNC in tH(bb̄).

TOP-21-004 tt̄γ xsec.

Higgs measurements

HIG-20-007 **Anomalous Higgs couplings to vector bosons/fermions in production using H->ττ final state**.

HIG-21-013 Off-shell Higgs production and anomalous couplings.

ElectroWeak measurements

SMP-20-011 Double-differential inclusive jet xsec.

*Since last LHC EFTwg general meeting, May 2021.

t(t)Z: probing EFT operators with ML techniques in multilepton final states.

(TOP-21-001, arXiv:2107.13896 - sub.to JHEP)

Overview

- Target 3 t-Z associated production modes, in 3 and 4 lep. final states:
  - highest-trigger efficiency (combined~100%)
  - favorable SNR
- EFT appealing phase-space
  - Top couplings to Z / γ / H not much constrained (compared to tW, tg)
- Most EFT operators modify the final state kinematics non-trivially
  - Use Machine Learning (ML) techniques to optimize the sensitivity to EFT

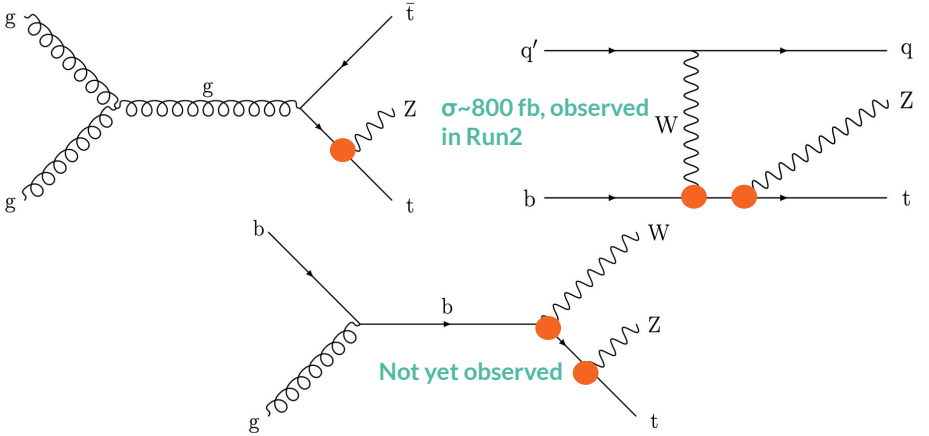

Considered diagrams including at most one EFT vertex, in which top is produced.

EFT signal modelling

Focus on a subset of five CP-conserving dimension-6 operators, modifying the tZ coupling at tree level

Operator	WC	Mapping to Warsaw-basis coefficients
$\mathcal{O}_{tZ}$	c_{tZ}	$\mathrm{Re}\{-s_W c_{uB}^{(33)} + c_W c_{uW}^{(33)}\}$
$\mathcal{O}_{tW}$	c_{tW}	$\mathrm{Re}\{c_{uW}^{(33)}\}$
$\mathcal{O}_{\varphi Q}^{3}$	$c_{\varphi Q}^{3}$	$c_{\varphi q}^{3(33)}$
$\mathcal{O}_{\varphi Q}^{-}$	$c_{\varphi Q}^{-}$	$c_{\varphi q}^{1(33)} - c_{\varphi q}^{3(33)}$
$\mathcal{O}_{\varphi t}$	$c_{\varphi t}$	$c_{\varphi u}^{(33)}$

Madgraph@LO SM+EFT samples.

- ★ EFT effects simulated with **dim6top** UFO model, included via reweighting.
- ★ Full detector simulation.
- ★ Extra parton included in simulation of $t\bar{t}Z$ to better describe NLO.

$$\mathcal{M} = \mathcal{M}_{SM} + \mathcal{M}_{EFT} = \mathcal{M}_{SM} + \sum_i c_i \cdot \mathcal{M}_i$$

$$w(\frac{\vec{c}}{\Lambda^2}) = S_0 + \sum_j S_{1,j}\frac{c_j}{\Lambda^2} + \sum_j S_{2,j}\frac{c_j^2}{\Lambda^4} + \sum_{j,k} S_{3,jk}\frac{c_j}{\Lambda^2}\frac{c_k}{\Lambda^2} \rightarrow \text{WC}$$

Coefficients to determine per event

SM | SM-EFT interference | Pure-EFT (quadratic) | EFT-EFT interference

1) Reweight generator-level events according to many different EFT scenarios

2) Perform per-event quadratic fit → Extract dependence of each event weight on each WC

3) Parameterization → Reweight any distribution according to any EFT scenario

➔ Cross sections & kinematics of signal samples parameterized with a five-dimensional quadratic function of the Wilson coefficients.

Bkgs & strategy

Events with a Z boson and at least one top quark leptonically decaying.

Baseline selection:

- ★ Veto presence of loose lepton pair with m(ll) < 12 GeV
- ★ ≥3 tight leptons with p_T >25/15/10 GeV
- ★ ≥ 1 Z boson candidate

Define 4 regions enriched in signals & main backgrounds

Selection requirement	SR-3ℓ	SR-t$\bar{t}$Z-4ℓ	WZ CR	ZZ CR
Lepton multiplicity	=3	=4	=3	=4
$m_{3\ell} - m_Z$	—	—	>15 GeV	—
Z boson candidates multiplicity	=1	=1	=1	=2
Jet multiplicity	≥2	≥2	—	—
b jet multiplicity	≥1	≥1	=0	—
p_T^{miss}	—	—	>50 GeV	—

➔ SR-3l drives the analysis sensitivity.

➔ SR-3l is further divided via multiclass discriminator output (next slide).

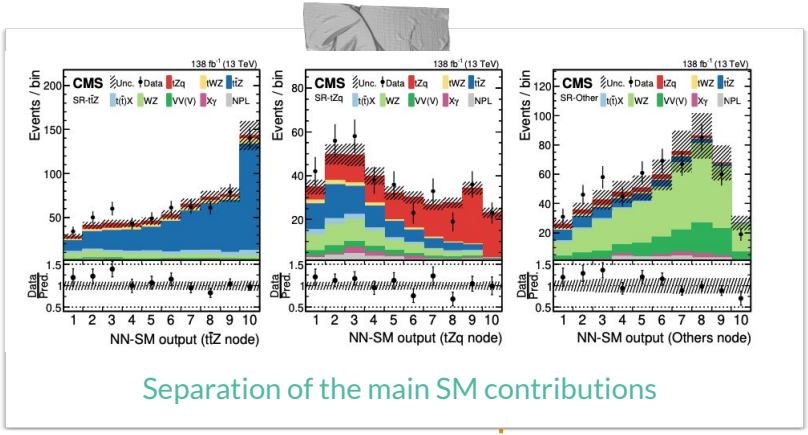

Separation of the main SM contributions

- SM-EFT interference included in training for first time in full-fledged analysis at LHC .
- Trained 8 NN-EFTs algorithms (targeting individual WCs with separate trainings, and the tZq and ttZ signals separately).

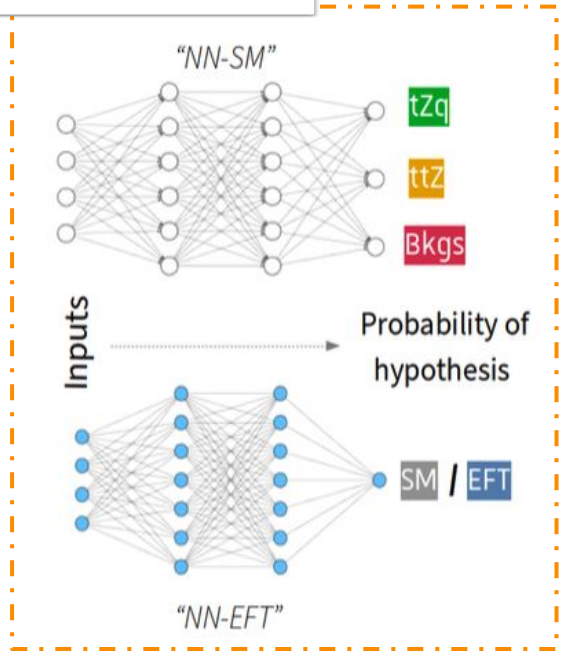

ML classification used for two purposes.

- Separate physics processes of interest in the signal region from backgrounds and from each other:
  - multiclass classifier trained to separate tZq/ttZ/others.
- Separate SM / EFT scenarios:
  - binary classifier to separate events SM hyp./non-zero WC like.

Signal extraction

Simultaneous template fits in 6 regions (3*sr3l+sr4l+WZcr+ZZcr) per year, testing 1D, 2D, or 5D WCs fit.

Different observables used in SR-tZq/SR-t$\bar{t}$Z depending on the number of parameter of interest and on WCs probed.

Signal yields parameterized with EFT in each bin to constrain WCs directly in the fits.

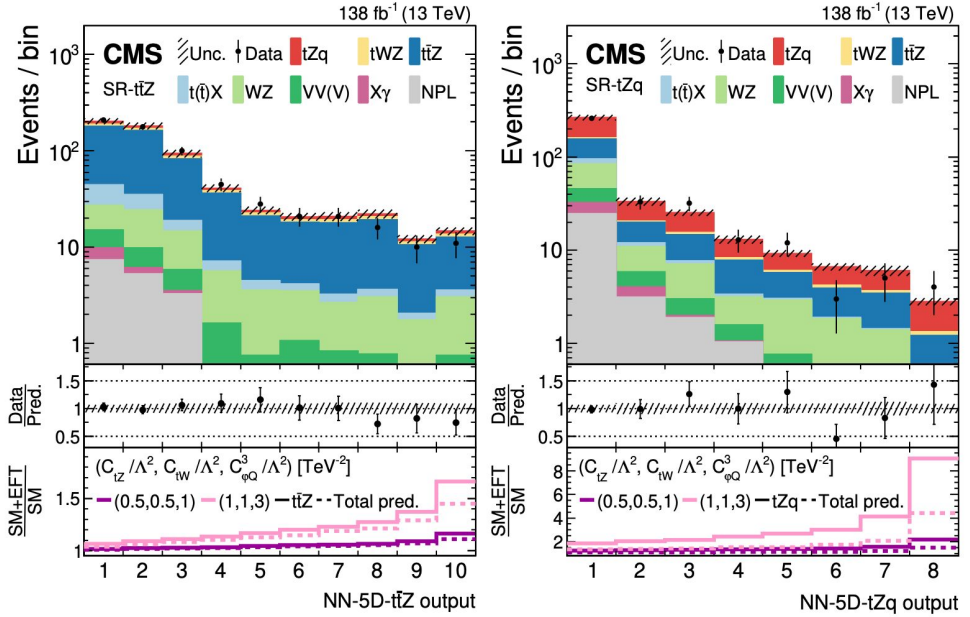

Separate trainings for 1D & 5D.

Fit configuration	Region					
	SR-tZq	SR-t$\bar{t}$Z	SR-Others	SR-t$\bar{t}$Z-4ℓ	CR WZ	CR ZZ
1D c_{tZ}	NN-c_{tZ}-tZq	NN-c_{tZ}-t$\bar{t}$Z				
1D c_{tW}	NN-c_{tW}-tZq	NN-c_{tW}-t$\bar{t}$Z				
1D $c^3_{\varphi Q}$	NN-$c^3_{\varphi Q}$-tZq	NN-$c^3_{\varphi Q}$-t$\bar{t}$Z				
1D $c^-_{\varphi Q}$	NN-SM (tZq node)	NN-SM (t$\bar{t}$Z node)	m_T^W	Counting experiments		
1D $c_{\varphi t}$	NN-SM (tZq node)	NN-SM (t$\bar{t}$Z node)				
2D and 5D	NN-5D-tZq	NN-5D-t$\bar{t}$Z				

Results (1).

- ➔ 1D likelihood scan as a function of each Wilson coefficient (other WCs fixed to 0).
- ➔ 5D confidence intervals at 95 % CL for each WC, in which all five WCs are treated as free parameters.

WC/Λ^2 $[TeV^{-2}]$	95% CL confidence intervals			
	Other WCs fixed to SM		5D fit	
	Expected	Observed	Expected	Observed
c_{tZ}	$[-0.97, 0.96]$	$[-0.76, 0.71]$	$[-1.24, 1.17]$	$[-0.85, 0.76]$
c_{tW}	$[-0.76, 0.74]$	$[-0.52, 0.52]$	$[-0.96, 0.93]$	$[-0.69, 0.70]$
$c^3_{\varphi Q}$	$[-1.39, 1.25]$	$[-1.10, 1.41]$	$[-1.91, 1.36]$	$[-1.26, 1.43]$
$c^-_{\varphi Q}$	$[-2.86, 2.33]$	$[-3.00, 2.29]$	$[-6.06, 14.09]$	$[-7.09, 14.76]$
$c_{\varphi t}$	$[-3.70, 3.71]$	$[-21.65, -14.61] \cup [-2.06, 2.69]$	$[-16.18, 10.46]$	$[-19.15, 10.34]$

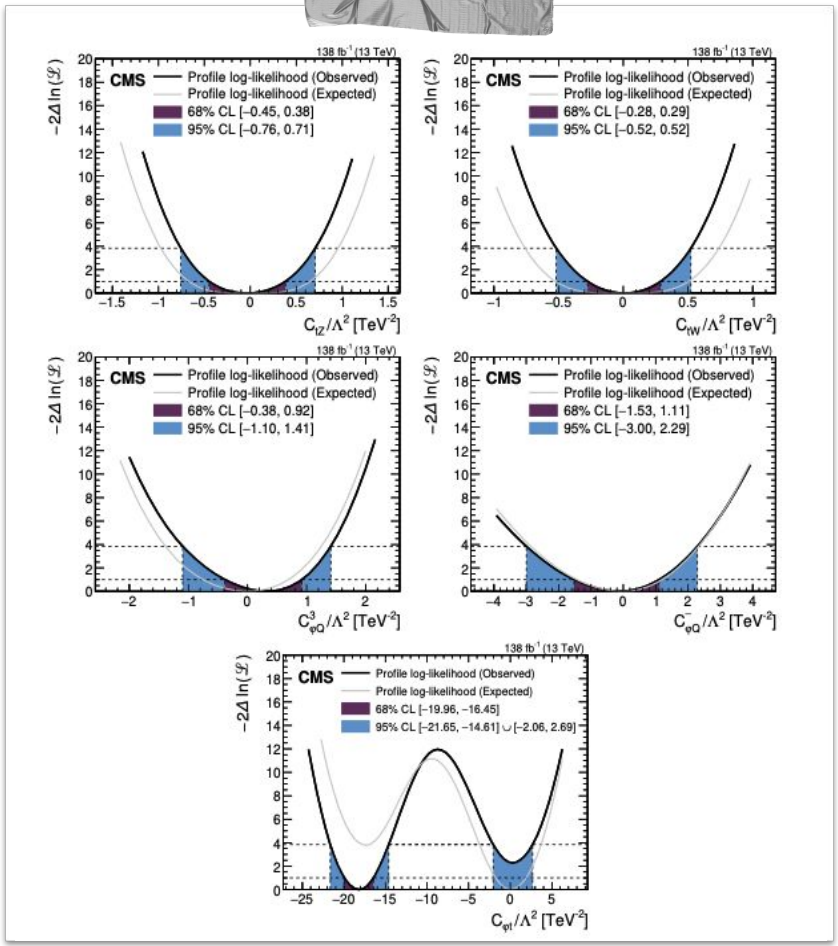

Results (2).

2D likelihood scans illustrate correlations of pairs of WCs (other WCs fixed to 0).

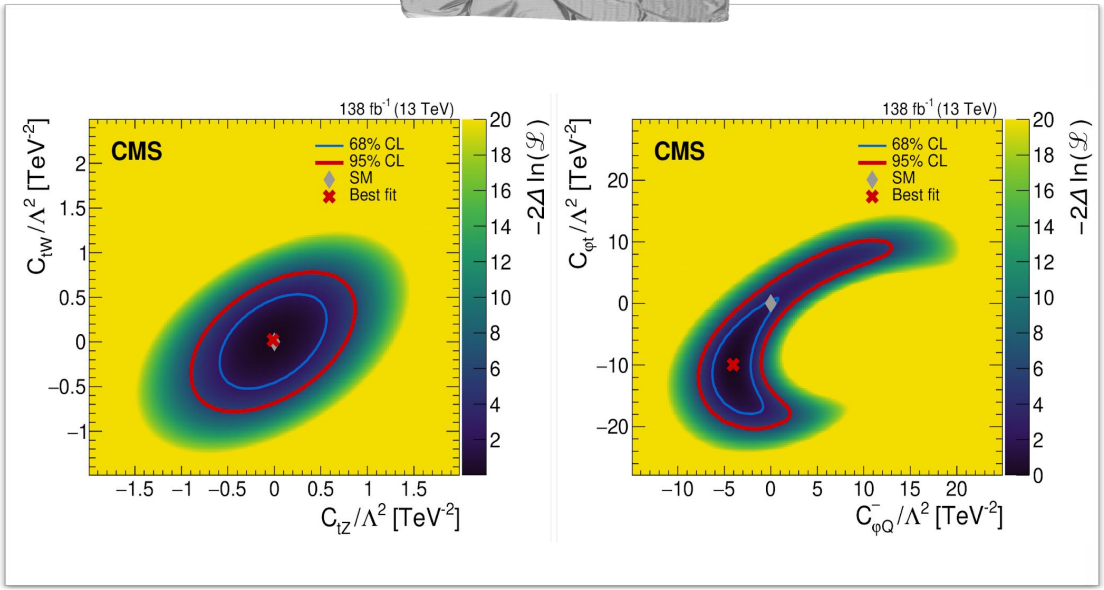

- ➔ Best direct constraints to date from multilepton final states on several coefficients.
- ➔ Significant sensitivity gains from shape information:
  - ◆ Shape information reduces widths of confidence intervals by ~20 % up to 70 %.
- ➔ All intervals contain the SM prediction.

$H \rightarrow \tau\tau$: probing anomalous coupling in production.

(HIG-20-007)

Anomalous H production

Are there any anomalous interactions between a Higgs boson and two gauge bosons? Current precision allows small anomalous CP-even and/or CP-odd couplings.

Higgs boson production in association with two jets:

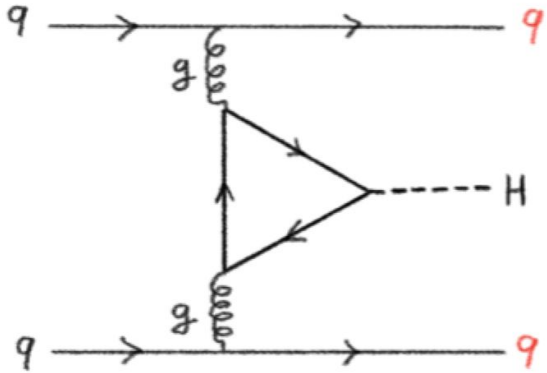

Second order ggH production.

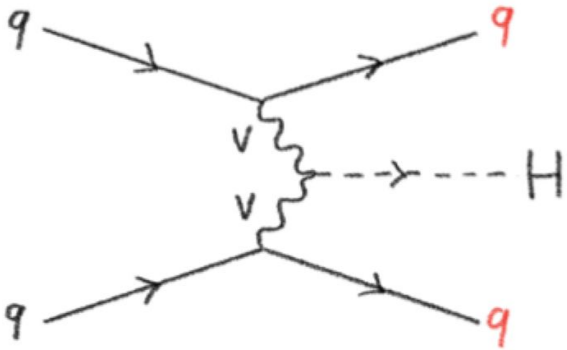

Tree level VBF production.

➔ H→ττ decay is important to measure anomalous couplings using these productions.

➔ The analysis uses matrix element likelihood approach (MELA), and a neural network to measurement of anomalous couplings (AC).

Anomalous H production

Generic spin-0 HVV scattering amplitude:

$$\mathcal{A}(\mathrm{HVV}) \sim \left[a_1^{\mathrm{VV}} + \frac{\kappa_1^{\mathrm{VV}} q_1^2 + \kappa_2^{\mathrm{VV}} q_2^2}{\left(\Lambda_1^{\mathrm{VV}}\right)^2} \right] m_{\mathrm{V1}}^2 \epsilon_{\mathrm{V1}}^* \epsilon_{\mathrm{V2}}^* + a_2^{\mathrm{VV}} f_{\mu\nu}^{*(1)} f^{*(2)\mu\nu} + a_3^{\mathrm{VV}} f_{\mu\nu}^{*(1)} \tilde{f}^{*(2)\mu\nu}$$

- considerations of symmetry and gauge invariance require:

$$a_1^{Z\gamma} = a_1^{\gamma\gamma} = a_1^{gg} = 0,\ \kappa_1^{ZZ} = \kappa_2^{ZZ},\ \kappa_1^{\gamma\gamma} = \kappa_2^{\gamma\gamma} = 0,\ \kappa_1^{gg} = \kappa_2^{gg} = 0$$

For the V=W,Z we are left with:

$a_1^{WW,ZZ}$ = CP-even couplings (SM-like)

$a_2^{WW,ZZ}$, $\kappa_1^{WW,ZZ}/(\Lambda_1^{WW,ZZ})^2$, $\kappa_2^{Z\gamma}/(\Lambda_1^{Z\gamma})^2$ = CP-even anomalous couplings

$a_3^{WW,ZZ}$ = CP-odd coupling

$a_1^{ZZ} = a_1^{WW}$ due to custodial symmetry

We consider two approaches to relate ZZ and WW couplings:

Approach 1: $a_i^{ZZ} = a_i^{WW}$, $\kappa_1^{ZZ}/(\Lambda_1^{ZZ})^2 = \kappa_1^{WW}/(\Lambda_1^{WW})^2$

Approach 2: $a_3^{WW} = \cos^2\theta_W\, a_3^{ZZ}$

Parametrization of Scattering Amplitudes:

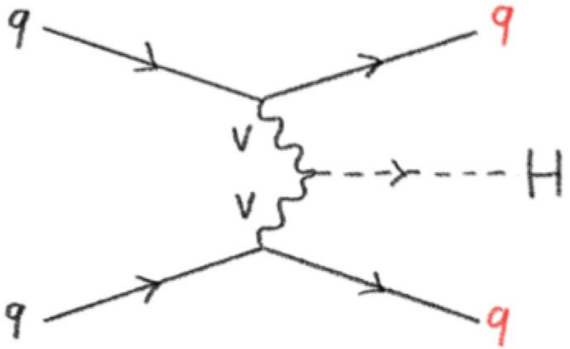

Convenient to parameterise ACs in terms of effective cross-sections (most of the uncertainties cancel in the ratio):

$$f_{ai} = \frac{|a_i|^2 \sigma_i}{|a_1|^2\sigma_1 + |a_2|^2\sigma_2 + |a_3|^2\sigma_3 + |\kappa_1|^2\sigma_{\Lambda 1} + |\kappa_1^{Z\gamma}|^2\sigma_{\Lambda 1}^{Z\gamma}} \operatorname{sgn}\left(\frac{a_i}{a_1}\right)$$ (for V=W,Z)

Anomalous H production

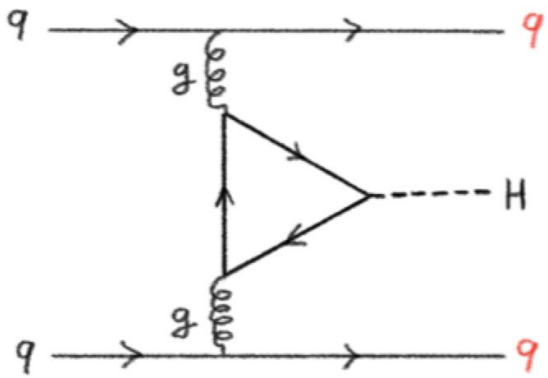

Parametrization of Scattering Amplitudes:

Generic Hff scattering amplitude:

$$\mathcal{A}(\mathrm{Hff}) = -\frac{m_f}{v}\bar{\psi}_f\left(\kappa_f + i\tilde{\kappa}_f\gamma_5\right)\psi_f$$

κ_f = CP-even coupling (SM-like)

$\tilde{\kappa}_f$ = CP-odd coupling

Can define fraction or effective mixing angle

$$f_{CP}^{Hff} = \frac{|\tilde{\kappa}_f|^2}{|\kappa_f|^2 + |\tilde{\kappa}_f|^2}\,\mathrm{sgn}\left(\frac{\tilde{\kappa}_f}{\kappa_f}\right) \qquad \alpha^{Hff} = \tan^{-1}\left(\frac{\tilde{\kappa}_f}{\kappa_f}\right)$$

Assuming only top and bottom contribute to the ggH loop and $\kappa_t=\kappa_b=\kappa_f$ and $\tilde{\kappa}_t=\tilde{\kappa}_b=\tilde{\kappa}_f$ [arXiv:2002.09888]

$$\left|f_{CP}^{Hff}\right| = \left(1 + 2.38\left[\frac{1}{\left|f_{a3}^{ggH}\right|} - 1\right]\right)^{-1}$$

Analysis strategy

Targeting VBF and ggH events, via four H→$\tau\tau$ decay channels: $\tau_h\tau_h$, μτ_h, eτ_h, and eμ

➔ Kinematics of Higgs and associated jets sensitive to ACs:

- VBF results extracted by fitting MELA-based observables,
- ggH results extracted with both MELA & simplified observables.

3 categories based on production modes:

➔ 0-Jet: No jets with pT > 30 GeV.

➔ VBF: 2 or more jets with m(jj) > 300 GeV ($|\Delta\eta|_{jj}$ > 2.5 and pTH>100 GeV) for the eτ_h, μτ_h, and eμ ($\tau_h\tau_h$) channels.

➔ Boosted: 1-jets events or 2+ jets events failing VBF cuts - selects boosted ggH+j events, VH, and some VBF.

VBF category drives ACs sensitivity

Kinematics and discriminants

From the 7 observables (Ω) that fully describe the topology

MELA reduction to 3 types of discriminant:

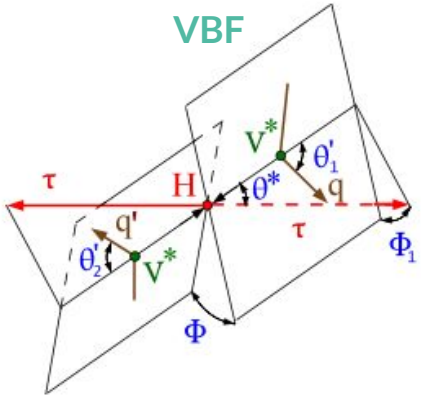

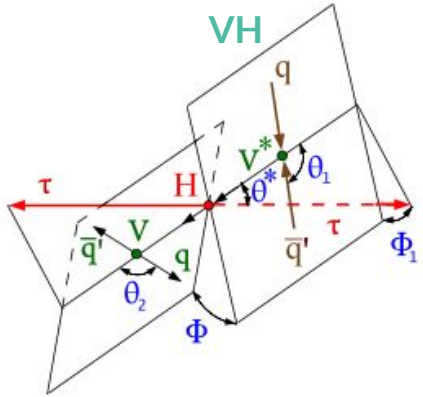

Separate SM from pure/quadratic BSM contributions.

Sensitive to interference btw SM and BSM couplings.

Separate ggH from VBF.

$$\mathscr{D}_{\rm BSM} = \frac{\mathscr{P}_{\rm SM}(\vec{\Omega})}{\mathscr{P}_{\rm SM}(\vec{\Omega}) + \mathscr{P}_{\rm BSM}(\vec{\Omega})}$$

$$\mathscr{D}_{\rm int} = \frac{\mathscr{P}^{\rm int}_{\rm SM-BSM}(\vec{\Omega})}{\mathscr{P}_{\rm SM}(\vec{\Omega}) + \mathscr{P}_{\rm BSM}(\vec{\Omega})}$$

$$\mathscr{D}^{\rm VBF}_{\rm 2jet} = \frac{\mathscr{P}^{\rm ggH}_{\rm SM} + \mathscr{P}^{\rm ggH}_{\rm 0-}}{\mathscr{P}^{\rm ggH}_{\rm SM} + \mathscr{P}^{\rm ggH}_{\rm 0-} + \mathscr{P}^{\rm VBF}_{\rm SM}}$$

★ $\mathscr{P}_i$ is the probability for the process (i=SM, BSM).

★ $\mathscr{P}_{\rm SM-BSM}$ is the interference part of the probability distribution with a mixture of SM and BSM.

➔ 1 $\mathscr{D}_{\rm BSM}$ observable per f_{ai} that we measure.

➔ For CP-odd parameters we include also $\mathscr{D}_{\rm int}$.

Signal extraction & results

- Binned maximum likelihood fit combining all categories: separate fits per each AC.
- In the VBF and VH production analysis, constraints on the CP-violating parameter f_{a3} and on the CP-conserving parameters f_{a2}, $f_{\Lambda 1}$, and $f_{Z\gamma}$.
- In ggH constraints set on the CP violating effects in terms of the effective cross section ratio f^{ggH} and mixing angle α_{Hff}.

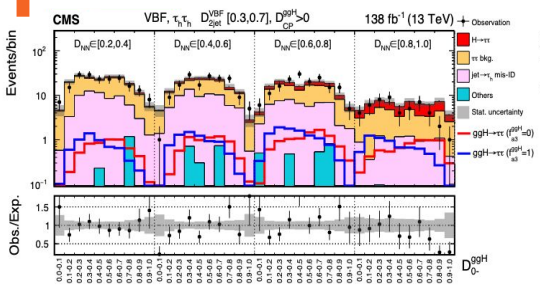

f_{a3}^{ggH} fit using MELA-method

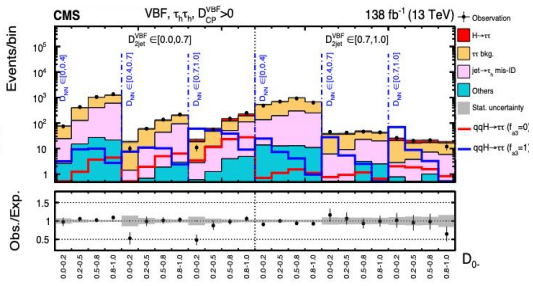

f_{a3} fit using MELA-method

Approach	Parameter	Observed / (10^{-3})		Expected / (10^{-3})	
		68% CL	95% CL	68% CL	95% CL
Approach 1	f_{a3}	$0.26^{+0.38}_{-0.21}$	$[-0.01, 1.30]$	0.00 ± 0.06	$[-0.23, 0.23]$
	f_{a2}	$1.1^{+0.9}_{-0.9} \cup [-1.8, -0.1]$	$[-3.4, 3.2]$	$0.0^{+0.6}_{-0.5}$	$[-1.4, 1.5]$
	$f_{\Lambda 1}$	$-0.12^{+0.08}_{-0.10}$	$[-0.34, 0.01]$	$0.00^{+0.19}_{-0.05}$	$[-0.15, 0.55]$
	$f_{\Lambda 1}^{Z\gamma}$	$2.5^{+1.8}_{-1.8}$	$[-3.6, 6.5]$	$0.0^{+1.5}_{-1.2}$	$[-3.2, 3.4]$
Approach 2	f_{a3}	$0.40^{+0.53}_{-0.33}$	$[-0.01, 1.90]$	0.00 ± 0.08	$[-0.33, 0.33]$

Parameter	Method	Observed		Expected	
		68% CL	95% CL	68% CL	95% CL
f_{a3}^{ggH}	MELA	$0.08^{+0.35}_{-0.08}$	$[-0.09, 0.90]$	0.00 ± 0.36	-
f_{a3}^{ggH}	$\Delta\phi_{jj}$	$0.07^{+0.59}_{-0.19}$	-	0.00 ± 0.39	-
α^{Hff}	MELA	$11^{+18\circ}_{-10}$	$[-11, 63]$	$0 \pm 26^\circ$	-
α^{Hff}	$\Delta\phi_{jj}$	$10^{+32\circ}_{-24}$	-	$0 \pm 27^\circ$	-

Combined results*

Combination of H → ττ with the Run 2 analyses H →ZZ→ 4l, and H → γγ

HVV

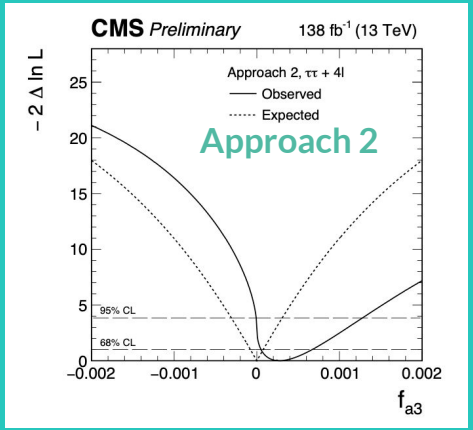

ggH

First exclusion of the pure CP-odd ggH coupling scenario with a significance >2σ.

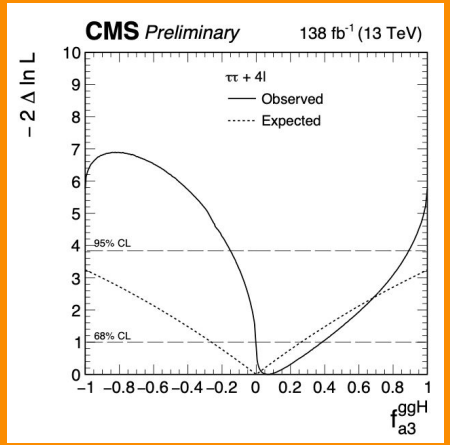

Htt

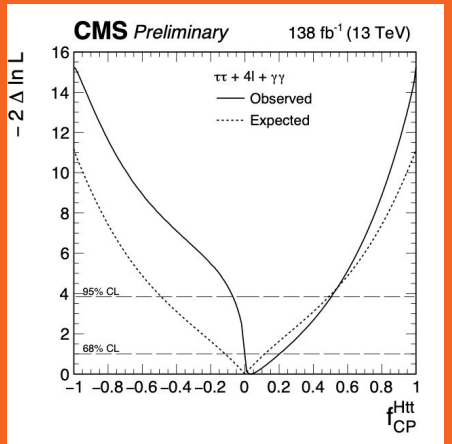

The combination improves the limits on the anomalous coupling parameters typically by about 20–50%.

Conversion to EFT bounds

- EFT parameters conversion to Higgs basis:

$$c_{gg} = -\frac{1}{2\pi\alpha_S} a_2^{gg}$$

$$\tilde{c}_{gg} = -\frac{1}{2\pi\alpha_S} a_3^{gg}$$

- + accounting for EFT separate couplings for top (kt and kt~) in two distinct fitting procedures:
  - Top: kt and kt~ floated,
  - Bottom: kt and kt~ fixed to SM.

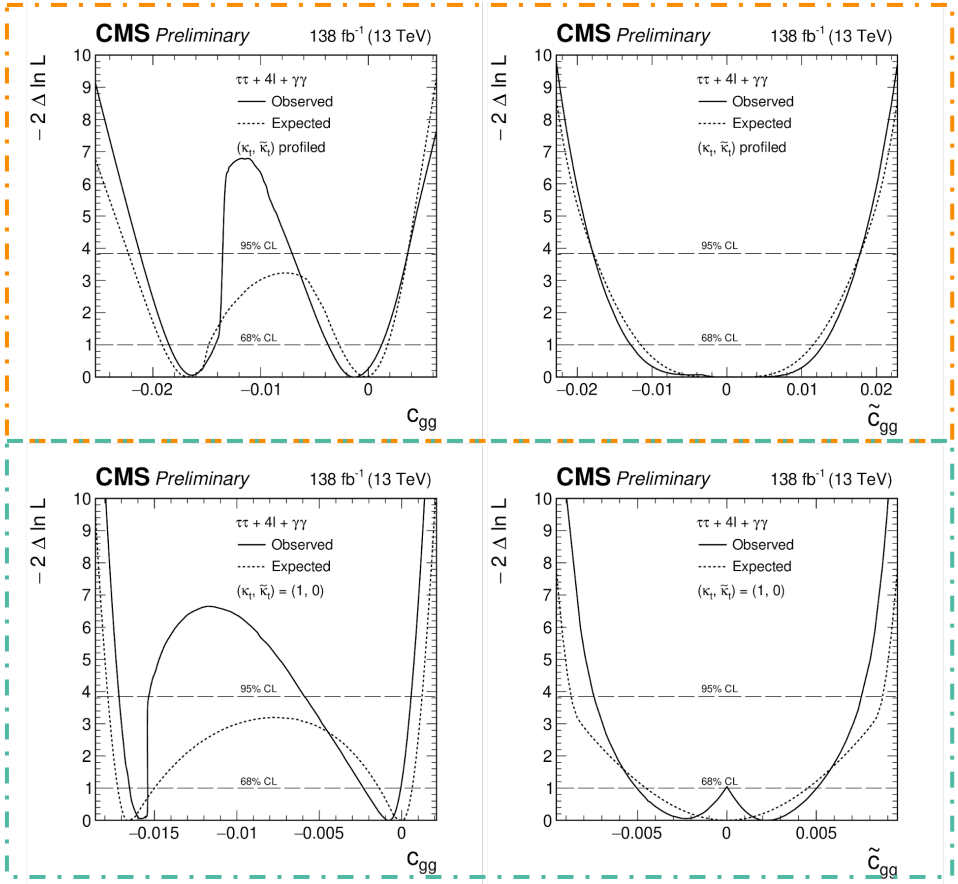

Summary.

- ➔ Novel approach with ML potentiality in EFT search:
  - ◆ EFT effects parameterized at detector-level via event weights.
  - ◆ Obtain best direct limits to date from multilepton final states on several Wilson coefficients.

- ➔ Search for anomalous effects, in the tensor structure of the H interactions with electroweak bosons (HVV) and gluons (Hgg):
  - ◆ matrix element likelihood approach and a neural network to optimize the measurement of anomalous couplings, as well as interpretation in terms of EFT scenario.

Thank you.

To the memory of our EFT enthusiast Nicolas Tonon.

BACKUP

Variable	NN-SM	NN-c_{tZ}-tZq	NN-c_{tZ}-t$\bar{t}$Z	NN-c_{tW}-tZq	NN-c_{tW}-t$\bar{t}$Z	NN-$c^3_{\varphi Q}$-tZq	NN-$c^3_{\varphi Q}$-t$\bar{t}$Z	NN-5D-tZq	NN-5D-t$\bar{t}$Z
p_T^Z	—	✓	✓	✓	✓	✓	✓	✓	✓
$\eta(Z)$	✓	✓	✓	—	—	✓	—	—	✓
$\Delta\phi(\ell_1^Z\ell_2^Z)$	✓	✓	✓	✓	✓	✓	✓	✓	✓
$p_T(t)$	✓	✓	✓	—	✓	✓	—	✓	✓
$\eta(t)$	—	✓	✓	✓	✓	✓	—	—	✓
$m(t,Z)$	—	—	—	—	—	—	—	—	—
$\lvert\eta(j')\rvert$	✓	—	—	—	—	—	—	✓	—
$p_T(j')$	✓	✓	—	✓	—	—	—	—	—
$\Delta R(b,\ell_t)$	—	✓	—	✓	—	—	—	—	—
$\Delta R(j',\ell_t)$	✓	—	—	—	—	—	—	—	—
$\Delta R(t,Z)$	—	✓	✓	✓	—	✓	—	—	✓
$\Delta\eta(Z,j')$	—	✓	—	—	—	—	—	✓	—
ΔR between t and the closest lepton	—	✓	—	✓	—	—	—	—	—
ΔR between j' and the closest lepton	—	—	—	—	—	—	—	✓	—
$m_{3\ell}$	✓	—	—	—	✓	—	✓	—	✓
m_T^W	✓	✓	✓	—	—	—	—	—	✓
p_T^{miss}	✓	—	—	—	—	—	—	—	—
Lepton asymmetry	✓	—	—	✓	✓	—	—	✓	—
$\cos\theta_Z^\star$	—	—	✓	—	—	✓	—	—	✓
Max. p_T among jet pairs	—	—	—	—	—	—	✓	—	✓
Max. DEEPJET discriminant	✓	—	—	—	—	—	—	—	—
b jet multiplicity	✓	—	—	—	—	—	—	—	—
Three-momenta of the three leading leptons	✓	—	—	—	—	—	—	—	—
Three-momenta of the three leading jets	✓	—	—	—	—	—	—	—	—
DEEPJET discriminants of the three leading jets	✓	—	—	—	—	—	—	—	—
Number of variables	33	11	8	8	6	7	4	7	10

TOP-21-001

Input variables to the NN-SM and to the eight NN-EFTs.

Source	c_{tZ}	c_{tW}	t	$c^{-}_{\varphi Q}$	$c_{\varphi t}$
tZq normalization	<0.1	<0.1	1.2	0.1	0.8
$t\bar{t}Z$ normalization	0.6	<0.1	0.4	37	38
tWZ normalization	0.1	0.1	<0.1	0.7	2.1
Background normalizations	<0.1	<0.1	6.9	3.6	6.8
NPL background estimation	1.4	0.2	5.6	0.3	3.8
Jet energy scale	<0.1	<0.1	0.8	0.7	2.3
Jet energy resolution	<0.1	<0.1	<0.1	<0.1	1.4
p_{T}^{miss}	<0.1	<0.1	<0.1	<0.1	0.2
b tagging	<0.1	<0.1	0.9	2.0	0.3
Other (experimental)	<0.1	<0.1	1.6	0.8	0.6
Lepton identification and isolation	0.4	0.4	1.2	2.2	0.8
Theory	2.1	1.1	0.4	0.9	0.9

TOP-21-001

Impacts from different groups of sources of systematic uncertainty on each individual WC.

- Dominant background in the analysis is from genuine di-τ pairs
  - Mainly coming from $Z \to \tau\tau$, but a smaller contribution from $t\bar{t}$ and diboson
- Second largest background is from jet$\to\tau_h$ misidentifications
- Minor backgrounds from diboson, $t\bar{t}$, $Z \to ll$
- Di-τ, jet$\to\tau_h$ backgrounds, and QCD (eμ) estimated from data
- Smaller background from MC
- Important for this analysis because:
  - Data-driven methods have very good statistics
  - Associated jets described very well

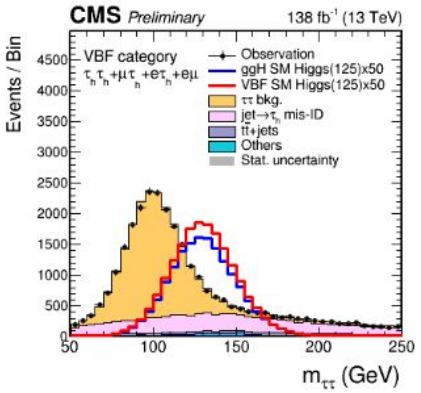

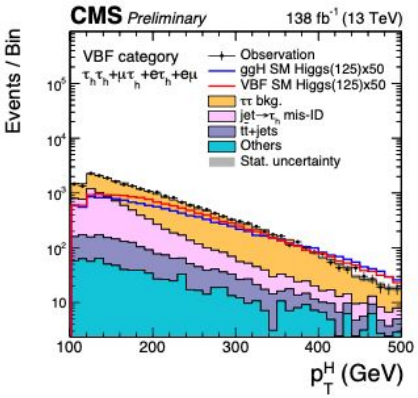

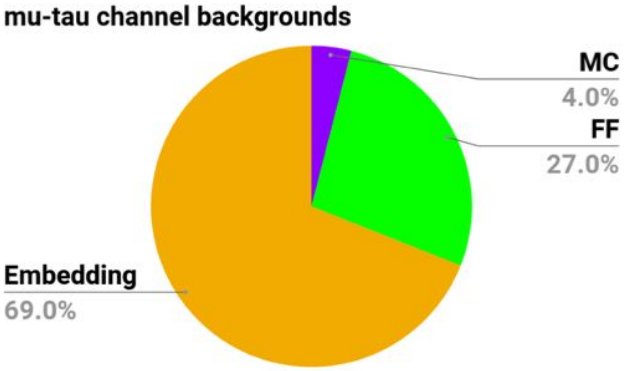

HIG-20-007

Overview of the backgrounds.

Uncertainty	Magnitude
τ_h ID	p_T/decay-mode dependent (2–3%)
τ_h separation from e/μ	3%
e $\to \tau_h$ ID	η dependent (9–40%)
$\mu \to \tau_h$ ID	η dependent (10–70)%
e ID	2%
μ ID	1%
b jet veto	0–10%
Luminosity	1.6%
Trigger	2% for e/μ, p_T/decay-mode dep. for τ_h ($\mathcal{O}(10\%)$)
$t\bar{t}$ cross section	4.2%
Diboson cross section	5%
Single top cross section	5%
Drell-Yan cross section	2%
L1 trigger timing (2016 and 2017)	Event-dependent (0.2–15%)
$\mathcal{B}(H \to \tau\tau)$	2.1%
τ_h energy scale	Decay-mode dependent (0.2–1.2%)
e $\to \tau_h$ energy scale	Decay-mode dependent (1–7%)
$\mu \to \tau_h$ energy scale	1%
Electron energy scale	p_T/η dependent ($< 1.25\%$)
Muon energy scale	η dependent 0.4–2.7%
Jet energy scale	p_T/η dependent ($\sim$ 0.5–14%)
Jet energy resolution	η dependent (2–95%)
p_T^{miss} unclustered energy scale	Event-dependent ($\sim$ 0–20%)
p_T^{miss} recoil corrections	0.3–5.8%
Jet $\to \tau_h$ mis-ID	Event-dependent ($\mathcal{O}(10\%)$)
QCD multijet in the eμ channel	Event-dependent ($\mathcal{O}(20\%)$)
Embedded yield	4%
$t\bar{t}$ in embedded	10%
Signal theoretical uncertainty	Event-dependent (up to $\sim$ 25%)
Top p_T reweighting	p_T dependent (0–21%)
DY p_T-mass reweighting	p_T/mass dependent (0–11%)

HIG-20-007

Impacts from different groups of sources of systematic uncertainty.